

acterization of three O-acetylated gangliosides from bovine buttermilk and their reactivity toward the monoclonal antibodies, D1.1 (5, 11), 18B8 (29), and A2B5 (30).

EXPERIMENTAL PROCEDURES

Materials—Bovine buttermilk powder was from Land O'Lakes (Minneapolis, MN). High performance TLC plates (nanoplates, 10 × 20 cm) were purchased from E. Merck, Darmstadt, Federal Republic of Germany. DEAE-Sephadex A-25 and Iatrobeads were from Pharmacia Fine Chemicals, Uppsala, Sweden, and Iatron Laboratories, Inc., Tokyo, Japan, respectively. The monoclonal antibody R24 was a generous gift from Dr. Kenneth Lloyd (Memorial Sloan-Kettering Cancer Center, New York, NY), the monoclonal antibody D1.1 was from Dr. Joel Levine (SUNY, Stony Brook, NY), and the monoclonal antibodies A2B5 and 18B8 were from Dr. George Grunwald (Jefferson Medical College, Philadelphia, PA). ¹²⁵I-Labeled staphylococcal protein A was supplied by Du Pont-New England Nuclear. Horseradish peroxidase-conjugated goat anti-mouse IgM or IgG was from Cappel, West Chester, PA. Anhydrous pyridine, hexamethyldisilazane, and trimethylchlorosilane were purchased from Pierce Chemical Co. All other chemicals were of HPLC or analytical grade.

Purification of Total Gangliosides—Bovine buttermilk powder, 1.7 kg, containing 32% protein, 8.5% minerals, 49% carbohydrates, and 3.5% other small molecular weight compounds, was suspended in water and then dialyzed against distilled water to remove small oligosaccharides, minerals, and other small molecular weight material. After lyophilization, 1 ml of 0.9% NaCl per g of dry dialyzed buttermilk powder was added to facilitate the ensuing extraction. The total lipids were extracted from the lyophilized materials with 10 volumes each of chloroform:methanol (C:M) (2:1, 1:1, and 1:2 v/v) (25). The combined lipid extracts were adjusted to a ratio of C:M:water (W) (2:1:0.6) and then partitioned three times (26). The ganglioside fractions from the upper phases were combined, evaporated, and dialyzed against deionized water for 3 days with frequent changing of water and then lyophilized. The residue containing gangliosides was dissolved in C:M:W (30:60:8) (solvent A) and applied onto a DEAE-Sephadex A-25 chromatographic column (100 × 2.0 cm, inside diameter). The column was washed with 10 volumes of solvent A to remove neutral lipids, then the crude gangliosides were eluted stepwise with a solvent system of 1,000 ml each of 0.05 M, 0.2 M, and 0.8 M sodium acetate in solvent A. One hundred eighty 15-ml effluent fractions were collected. On the basis of the elution profile, fractions 1–80 were pooled as monosialogangliosides, 80–110 as disialogangliosides, and 110–140 as trisialogangliosides. The solvent in each fraction was evaporated. After removing the sodium acetate in each fraction by dialysis, individual gangliosides in the di- and trisialoganglioside fractions were separated on a Iatrobeads column (100 × 2.0 cm) with gradient elution using 1 liter each of C:M:0.5% CaCl₂·2H₂O (70:30:3 and 35:65:5, v/v for disialogangliosides) or C:M:0.5% CaCl₂·2H₂O (60:40:5 and 35:65:10, v/v for trisialogangliosides).

Final purification of individual gangliosides was achieved by Iatrobeads column (110 × 0.4 cm) chromatography as follows. O-Acetylated G_{D3} was purified by gradient elution using C:M:W (70:30:3 and 35:65:5, v/v) and O-acetylated G_{T3} by gradient elution using C:M:W (65:35:5 and 30:70:10, v/v). The purity of each O-acetylated ganglioside species was examined by high performance thin layer chromatography (HPTLC) with two different solvent systems: (a) *n*-propyl alcohol:water (80:20, v/v) and (b) C:M:0.5% aqueous CaCl₂·2H₂O (55:45:10, v/v). The gangliosides were visualized on the plate by spraying with the resorcinol-HCl reagent (27) followed by heating at 95 °C for 30 min.

Mild Alkali Treatment of O-Acetylated Gangliosides—One hundred μg of a ganglioside sample was treated with 0.2 N methanolic NaOH at 37 °C for 2 h. The reaction mixture was then neutralized with 0.2 N HCl, and the salts in the mixture were removed by a Sephadex LH-20 column (47 × 0.5 cm, inside diameter; 23-ml bed volume) by elution with C:M:W (30:60:8).

HPTLC Overlay of O-Acetylated Gangliosides—HPTLC overlay was carried out according to Kasai *et al.* (28). Briefly, the gangliosides were chromatographed on an HPTLC plate with the developing solvent system of C:M:0.5% aqueous CaCl₂·2H₂O (55:45:10, v/v). After chromatography, the plate was dried *in vacuo* for 2 h and dipped in a solution of 0.4% poly(isobutyl methacrylate) in *n*-hexane for 1 min and dried *in vacuo*. The plate was incubated with 1% BSA in PBS (BSA/PBS) (pH 7.4) at room temperature for 90 min and then overlaid with monoclonal antibodies D1.1, A2B5, or 18B8 at a dilution of 1:50–100 in BSA/PBS. After incubation at room temperature for 90 min, the plate was washed with PBS five times. The plate overlaid with D1.1 was covered with horseradish peroxidase-conjugated goat anti-mouse IgM or IgG at a dilution of 1:100 in BSA/PBS for 90 min and washed as described above. After washing, the plate was incubated for a few minutes with 0.5 mg/ml 4-chloro-1-naphthol and 0.01% H₂O₂ as substrate.

The plates overlaid with A2B5 and 18B8 were covered by goat anti-mouse Ig at a dilution of 1:100 in BSA/PBS for 60 min. After washing with PBS, the plates were covered with 2 ml of ¹²⁵I-labeled staphylococcal protein A (10⁶ cpm/ml), incubated for 60 min, and washed with 0.1% Triton X-100 in 0.9% NaCl, followed by exposure to an x-ray film.

Compositional Analysis—To determine the sugar and fatty acid compositions, gas-liquid chromatographic (GLC) analysis was carried out according to the procedure of Ariga *et al.* (31) with slight modifications. A ganglioside sample, containing about 50 μg of sialic acid, was subjected to methanolysis for 18 h at 75 °C with 1 ml of 1% methanolic hydrogen chloride. Following methanolysis, the resulting fatty acid methyl esters were extracted with *n*-hexane, and the extract was evaporated and dissolved in 50 μl of *n*-hexane. An aliquot of this solution was injected onto a column of HP5 (cross-linked 5% PhMe Silicone, 25 m × 0.2 mm × 0.5 μm film thickness) maintained at 270 °C for analysis of fatty acids. The lower methanolic layer was evaporated under a stream of nitrogen and dried *in vacuo*. The dried residue was treated with 100 μl of hexamethyldisilazane:trimethylchlorosilane:pyridine (1.3:0.8:1, v/v) at 60 °C for 5 min, and the resulting trimethylsilylated derivatives of the saccharides were analyzed by GLC on the HP5 column programmed at 3 °C/min from 220 to 270 °C.

Fast-atom Bombardment (FAB) Mass Spectrometry—Negative ion FAB mass spectra were obtained by a TSQ 70 triple-stage quadrupole mass spectrometer (Finnegan MAT Inc., San Jose, CA) equipped with a FAB ion source. Xenon gas was used at 8 kV as an ionization beam. A ganglioside sample, 30 μg, was dissolved in 10 μl of C:M (1:1, v/v). Triethanolamine:tetramethylurea (1:1, v/v, 2 μl) was added, and the solvent mixture (about 1 μl) was applied to a stainless steel sample holder. The sample was analyzed as described previously (31).

Proton Nuclear Magnetic Resonance Spectroscopy—Samples were prepared for ¹H NMR analysis as described previously (32, 33). Briefly, each sample, 2 mg, was dissolved in 0.5 ml of D₂O and lyophilized to remove exchangeable protons. The residue was dissolved in 0.5 ml of dimethyl sulfoxide-*d*₆/D₂O (98:2, v/v). NMR spectra were obtained on spectrometers operating at ¹H frequencies of 300 MHz or 500 MHz.

Resonance assignments were made largely on the basis of a 300-MHz two-dimensional Homonuclear Hartman-Hahn spectroscopy (HOHAHA) data set which was acquired with a mixing time of 80 ms and a spin lock field strength of 8 kHz. This data set consisted of 384 *t*₁ increments. Each *t*₁ increment consisted of 1024 complex points over a 2401-Hz sweep width averaged for 256 transients with a 1.1 second repetition rate. Quadrature detection was achieved in the *f*₁ dimension using hypercomplex phase cycling with real and imaginary *t*₁ points stored separately. Data were processed for phase-sensitive display using FELIX 2.0 (Hare Research, Bothell, WA) with cosine bell weighing functions and zero filling in both dimensions to yield a 2K × 2K data matrix.

RESULTS

After Folch partitioning, 4.12 g of lipid extract were recovered from 0.67 kg of lyophilized materials after dialysis. About 360 mg of mono-, 680 mg of di-, and 196 mg of trisialoganglioside fractions were recovered from the DEAE-Sephadex A-25 column (see "Experimental Procedures"). Fig. 1 shows the elution profile for bovine buttermilk gangliosides. At least three alkali-labile gangliosides, which were designated as G₁, G₂, and G₃, could be detected on the basis of mild alkali

¹ The abbreviations used are: HPLC, high performance liquid chromatography; HPTLC, high performances thin layer chromatography; ¹H NMR, proton-nuclear magnetic resonance; HOHAHA, homonuclear Hartman-Hahn spectroscopy; FAB, fast-atom bombardment; BSA/PBS, bovine serum albumin in phosphate-buffered saline; mAb, monoclonal antibody. The ganglioside nomenclature follows the system of Svennerholm (1) and a recent IUPAC-IUB recommendation (2).

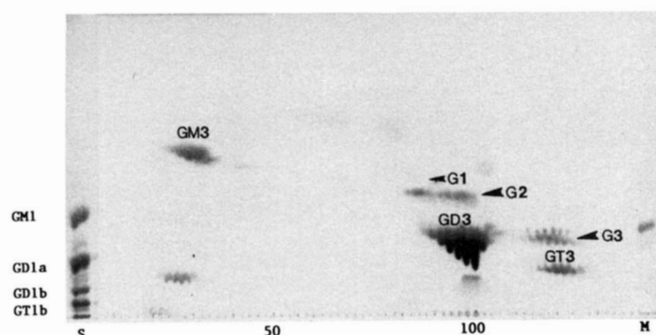


FIG. 1. HPTLC ganglioside profile of bovine buttermilk. The profile was obtained by eluting the gangliosides from a DEAE-Sephadex A-25 column. Two μ l from each of individual fractions were spotted on the plate. The developing solution was solvent system b (see "Experimental Procedures"). The spots were located with resorcinol-HCl reagent. Lane S, standard gangliosides; lane M, a mixture of gangliosides extracted from bovine buttermilk. Three acetylated gangliosides, designated as G₁, G₂, and G₃, were recognized on the profile.

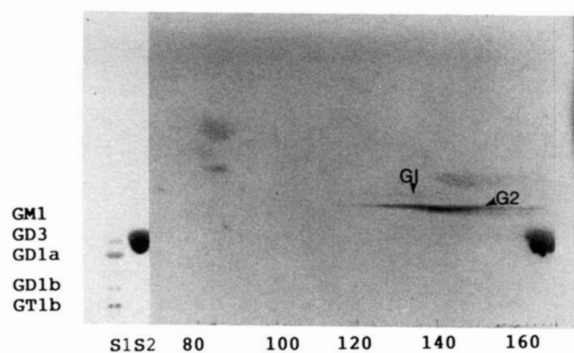


FIG. 2. HPTLC purification profiles of O-acetylated G_{D3} gangliosides from bovine buttermilk. O-Acetylated G_{D3} was purified from the disialoganglioside fraction by Iatrobeds column chromatography. The developing solution was solvent system b (see "Experimental Procedures"). The spots were located with resorcinol-HCl reagent. Lane S1, standard gangliosides; lane S2, standard ganglioside G_{D3}. O-Acetylated ganglioside G_{D3} was separated from G_{D3} and could be recognized on the plate.

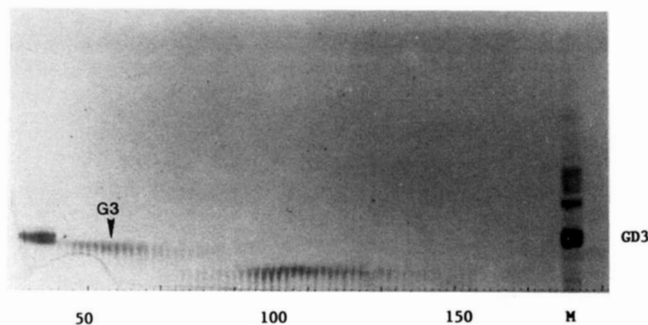


FIG. 3. HPTLC purification profiles of O-acetylated G_{T3} gangliosides from bovine buttermilk. O-Acetylated G_{T3} was separated from trisialoganglioside G_{T3}, which is around fraction 100, by Iatrobeds column chromatography. Other conditions were the same as described in Fig. 2.

treatment as described later. As previously reported (34), bovine buttermilk was found to contain 0.92 μ mol of lipid-bound sialic acid/g dry weight. The concentrations of acetylated gangliosides G₁, G₂, and G₃ are 0.4% (2 mg), 5% (37 mg), and 6% (40 mg) of the total lipid-bound sialic acid, respectively. Figs. 2 and 3 show the ganglioside elution profiles from Iatrobeds column chromatographies. Three gangliosides, G₁ to G₃, were isolated and purified to homogeneity. Ganglioside G₁ migrated slightly further than ganglioside G₂, while G₂

migrated between G_{M2} and G_{M1}, and G₃ between G_{D3} and G_{D1a}. Table I shows the results of compositional analysis of the carbohydrates and fatty acids of G_{D3}, G₁, G₂, G_{T3}, and G₃. Gangliosides G₁ and G₂ contain glucose, galactose, and sialic acid in a molar ratio of 1:1:2, and G₃, 1:1:3, respectively. The fatty acid composition of these gangliosides is shown in Table I. The major fatty acids were stearic, behenic, tricosanoic, and tetracosanoic acids.

The purified gangliosides, G₁ to G₃, were subjected to alkaline treatment (see "Experimental Procedures"). After mild alkaline treatment, the degradation products from gangliosides G₁ and G₂ co-migrated on TLC with authentic G_{D3}, while G₃ co-migrated with G_{T3}, as shown in Fig. 4. These data suggest that these alkali-labile gangliosides may contain O-acetylated sialic acid residues.

Fig. 5 shows the negative ion-FAB mass spectra and fragmentation diagrams of gangliosides G_{D3}, G₁, and G₂, which were isolated from bovine buttermilk. In the mass spectra of G_{D3} (Fig. 5A), G₁ (Fig. 5B), and G₃ (Fig. 5C), five ion groups are clearly discernible which arise from ceramide and ceramide-bearing fragment ions. In the mass spectrum of G_{D3}, the prominent molecular ions [M + Na - 2H]⁻ are clearly seen

TABLE I
Sugar and fatty acid compositions of gangliosides isolated from bovine buttermilk

	Gangliosides				
	G _{D3}	G ₁	G ₂	G ₃	G _{T3}
Sugars					
Glc	1	1	1	1	1
Gal	1.09	0.98	0.85	1.02	1.01
Sialic acid	2.16	1.79	1.85	2.98	2.87
Fatty acid (%)					
14:0	2	Trace	Trace	Trace	2.5
16:1	0	0	Trace	Trace	0
16:0	7.7	1.9	2.2	10.8	7.4
18:1	Trace	3.3	11.8	6.6	10.7
18:0	3.7	7.4	22.4	38.3	15.6
20:1	Trace	Trace	Trace	Trace	Trace
20:0	1.6	1.2	1.0	2.6	1.4
21:0	1.7	Trace	1.2	Trace	1.2
22:0	27.3	25.0	15.7	18.0	19.1
23:0	31.7	30.9	19.6	13.0	21.4
24:1	2.9	2.5	2.1	Trace	1.5
24:0	19.3	25.2	18.6	6.7	19.1
25:0	1.5	1.4	1	Trace	Trace

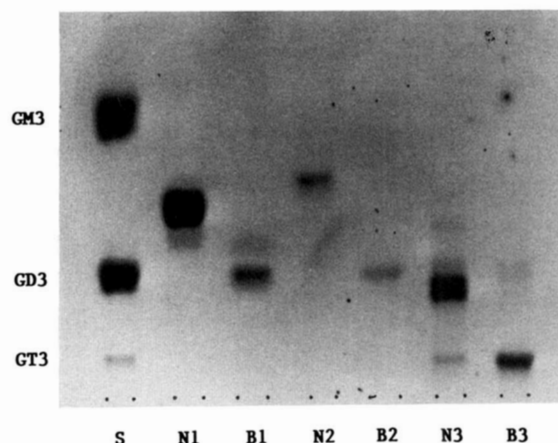


FIG. 4. HPTLC of purified O-acetylated gangliosides treated with methanolic NaOH. Lane 1, standard gangliosides; lanes N1, N2, and N3 correspond to untreated G₂, G₁, and G₃, respectively; lanes B1, B2, and B3 to treated G₂, G₁, and G₃, respectively. Other conditions were the same as described in Fig. 3. The bands were visualized by spraying with the resorcinol-HCl reagent.

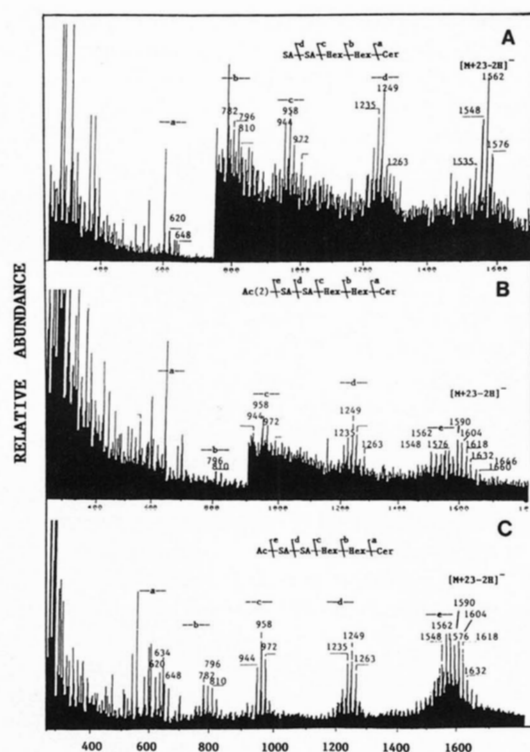


FIG. 5. The negative ion-FAB mass spectra and fragmentation diagrams of G_{D3} (A), G_1 (B), and G_2 (C).

in which the major ions at m/z 1548, 1562, and 1576 provide information on the molecular weights of G_{D3} molecular species with C18-sphingosine and C22:0, C23:0, and C24:0 fatty acids, respectively. These ions are also present in the spectra of G_1 and G_2 . However, the quasimolecular ions for G_1 and G_2 are shifted by 84 and 42 mass units from those observed for G_{D3} , respectively, suggesting the presence of two and one *O*-acetyl groups in G_1 and G_2 , respectively. For example, the ions at m/z 1632, 1646, and 1660 in G_1 correspond to di-*O*-acetyl G_{D3} ganglioside with C18-sphingosine and C22:0, C23:0, and C24:0 fatty acids, respectively. In the case of G_2 , these ions are of relatively low intensity, but the ions 1590, 1604, and 1618 are prominent, which provides information on the molecular weight of the monoacetyl G_{D3} molecular species.

In all spectra in Fig. 5, A, B, and C, the fragment ions corresponding to the formal elimination of 1 or 2 sialic acid units and 2 hexose units from the molecular ions are detected at m/z 1235, 1249, and 1263 (fragment group d), m/z 944, 958, and 972 (fragment group c), m/z 782, 796, and 810 (fragment group b), and m/z 620, 634, and 648 (fragment group a), respectively. Owing to the detection of three ions, m/z 1235, 1249, and 1263 in the spectra of both G_1 and G_2 (Figs. 5, B and C), the *O*-acetyl groups must be attached to the terminal sialic acid in the molecule.

Fig. 6 shows the FAB mass spectra of G_{T3} and G_3 . In both spectra, six major ion groups are present, which arise from ceramide and ceramide-bearing fragment ions. In both spectra, ion regions are complex, probably due to the presence of quasimolecular ions containing $[M - H]^-$ and $[M + Na - 2H]^-$. For example, prominent molecular ions $[M - H]^-$ are detected at m/z 1839, 1853, and 1867 which correspond to the molecular species with C18-sphingosine and C22:0, C23:0, and C24:0 fatty acid, respectively. The less prominent ions at m/z 1876 and 1890 correspond to $[M + Na - 2H]^-$ ions with C18-sphingosine and C23:0 and C24:0 fatty acids, respectively. In the spectra of G_3 , all these ions are shifted by 42 mass units; therefore, G_3 is supposed to be mono-*O*-acetyl

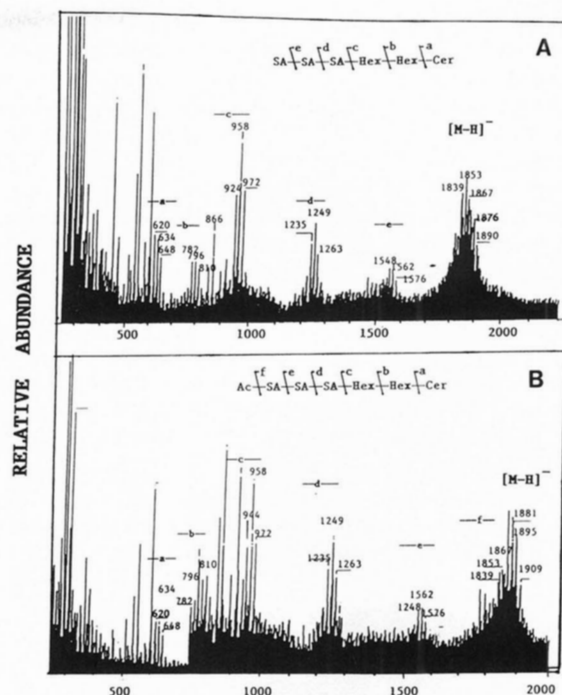


FIG. 6. The negative ion-FAB mass spectra and fragmentation diagrams of G_{T3} (A) and G_3 (B).

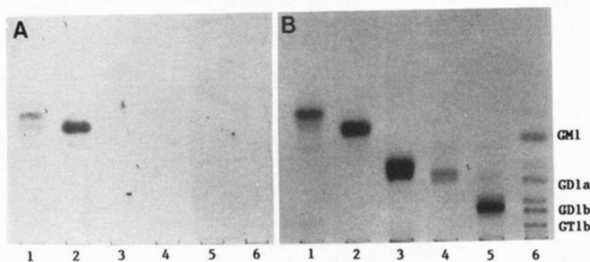


FIG. 7. Detection of *O*-acetylated ganglioside G_{D3} on HPTLC plate by immunoreactivity with monoclonal antibody D1.1. A, gangliosides reacting with monoclonal antibody D1.1 and horseradish peroxidase conjugate (see "Experimental Procedures"); B, gangliosides visualized with the resorcinol-HCl reagent. Lanes 1-5 correspond to G_1 , G_2 , G_{D3} , G_3 , and G_{T3} , respectively; lane 6, standard gangliosides. Each lane contains 2-5 μ g of lipid-bound sialic acid.

G_{T3} . In both spectra, three major fragment ions corresponding to the successive elimination of NeuAc (e), NeuAc (d), NeuAc (c), hexose (Gal) (b), and hexose (Glc) (a) are detected at m/z 1548, 1562, and 1576 for G_{D3} , m/z 1235, 1249, and 1263 for G_{M3} , m/z 944, 958, and 972 for LacCer, m/z 782, 796, and 810 for GlcCer, and m/z 620, 634, and 648 for ceramide, respectively. Since the ions m/z 1548, 1562, and 1576 corresponding to G_{D3} are not shifted, the *O*-acetyl group of G_{T3} must also be attached to the terminal sialic acid residue in the molecules.

In order to confirm the structures of the alkali-labile gangliosides, gangliosides G_1 , G_2 , and G_3 were analyzed by the HPTLC-overlay method using specific monoclonal antibodies against *O*-acetylated gangliosides. As shown in Figs. 7 and 8, G_1 and G_2 reacted with the monoclonal antibody D1.1 which is specific for 9-*O*-acetyl G_{D3} (14), and G_3 reacted with the monoclonal antibody A2B5 (29) but did not react with 18B8 which is specific for G_{T3} (30). The product of G_3 after mild alkaline treatment, however, reacted with 18B8. These data suggest that gangliosides G_1 and G_2 contain *O*-acetylated G_{D3} and G_3 is *O*-acetylated G_{T3} .

Although the mass spectrometric and immunochemical data provide clear evidence for the presence of both mono-

and di-*O*-acetylated gangliosides, these data cannot provide us with any information concerning the sites of *O*-acetyl substitution on the terminal α -NeuAc residue. Such data can be provided by nuclear magnetic resonance assignment data for these compounds as the chemical shifts of resonances corresponding to the sites of *O*-acetylation are likely to differ significantly from the same protons in the unsubstituted gangliosides. These resonance assignments, which were made on the basis of a two-dimensional HOHAHA data set, are summarized in Table II. In addition, the regions of the HOHAHA data set which contain the downfield shifted resonances corresponding to the sites of *O*-acetylation are provided in Fig. 9.

From the data in Table II and in Fig. 9, it is clear that the sample used for NMR analysis consisted of a mixture of mono- and disubstituted G_{D3} . In Fig. 9A, we present the region of the HOHAHA data set containing the downfield shifted resonances from the monosubstituted species (G_2). From these data, it is clear that there are two distinct monosubstituted species. In one species, the most striking feature was the

resonance at 4.82 ppm. This resonance was assigned to the H9b proton which is shifted downfield by more than 1 ppm from the H9b resonance position in unsubstituted G_{D3} . In addition, significant downfield shifts were noted for the H9a and H8 resonances. Based on these chemical shift differences, we conclude that this monosubstituted ganglioside corresponds to 9-*O*-Ac G_{D3} . In the other monosubstituted ganglioside, the most significant downfield shift is observed for the H7 resonance which is shifted to 4.15 ppm from its position at 3.21 ppm in unsubstituted G_{D3} . In addition, we noted a significant downfield shift for the H8 resonance in this ganglioside. On the basis of these shift differences, we conclude that this ganglioside corresponds to 7-*O*-Ac G_{D3} . Although shift perturbations were also noted for the H9a and H9b resonances in 7-*O*-Ac G_{D3} , these perturbations were somewhat smaller in magnitude than the perturbations noted for downfield shifts noted for the H9a and H9b resonances in 9-*O*-Ac G_{D3} . These data suggest that G_2 ganglioside is a mixture of 7-*O*-acetyl and 9-*O*-acetyl G_{D3} .

In Fig. 9B, we present the region of the two-dimensional HOHAHA data set containing the downfield shifted resonances for disubstituted species (G_1). Comparison of the data in Fig. 9B with the data shown in Fig. 9A shows that the spectrum of the di-*O*-acetyl species is similar to the spectrum which would be obtained by summing the spectra of the two mono-substituted G_{D3} species in Fig. 9A. These data are largely confirmed in the assignment data presented in Table II. In this ganglioside (G_1), we see large downfield shifts for the H7, H8, H9a, and H9b resonances. Therefore, we conclude that this diacetylated species corresponds to (7, 9)-di-*O*-Ac G_{D3} . Closer examination of the data in Table II indicates that the resonance positions for the H9a and H9b resonances are not identical with the positions observed in 9-*O*-Ac G_{D3} . These differences are likely indicative of some interaction between the two *O*-acetyl groups in the disubstituted species. Combined with the data from mobilities on HPTLC, mass spectrometric, and TLC immunostaining analysis, the results suggest a structure of G_1 most consistent with 7,9-di-*O*-acetyl G_{D3} (acetyl₂-*O*-7, 9NeuAc α 2 \rightarrow 8NeuAc α 2 \rightarrow 3Gal β 1 \rightarrow 4Glc β 1 \rightarrow

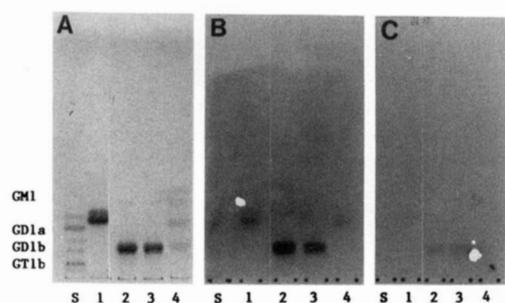


FIG. 8. Detection of *O*-acetylated ganglioside G_{T3} on HPTLC plate by immunoreactivity with the monoclonal antibodies A2B5 and 18B8 (see "Experimental Procedures"). A, the bands were visualized by spraying with the resorcinol reagent; B, gangliosides reacting with the monoclonal antibody A2B5; C, gangliosides reacting with the monoclonal antibody 18B8. Lanes 1, 2, 3, and 4 correspond to *O*-Ac G_{T3} (G_3), base-treated *O*-Ac G_{T3} (G_{T3}), G_{T3} , and a mixture of trisialogangliosides from bovine buttermilk, respectively; lane S, standard gangliosides. Each lane contains 2 μ g of lipid-bound sialic acid.

TABLE II
Chemical shifts for gangliosides G_{D3} and *O*-acetyl G_{D3}

	Residue								
	H-1	H-2	H-3	H-4	H-5	H-6	H-7	H-8	H-9
G_{D3}^a									
I.	4.16	3.05	3.31	3.28	3.28	3.60(a) 3.73(b)			
II.	4.27	3.28	3.63	3.87	3.35	3.45(a) 3.47(b)			
A.			1.69(a) 2.34(e)	3.83	3.57	3.14	3.43	3.43	3.55(a) 3.81(b)
C.			1.39(a) 2.77(e)	3.46	3.57	3.33	3.21	3.48	3.32(a) 3.58(b)
<i>O</i> -Ac G_{D3}									
I.	4.12	3.02	3.30	3.24	3.43	3.63(a) 3.71(b)			
II.	4.30	3.30	3.83						
A.			1.47(a) 2.35(e)	3.77	3.49	3.15	3.42	3.42	3.50(a) 3.80(b)
C.(7- <i>O</i> -)			1.40(a) 2.70(e)	3.49	3.39	3.28	4.15	3.92	3.15(a) 3.75(b)
(9- <i>O</i> -)			1.40(a) 2.70(e)	3.49	3.39	3.28	3.27	3.82	3.90(a) 4.82(b)
(7,9- <i>O</i> -)			1.40(a) 2.70(e)	3.49	3.39	3.28	4.26	4.06	3.69(a) 5.02(b)

^a Cited from Refs. 32 and 33.

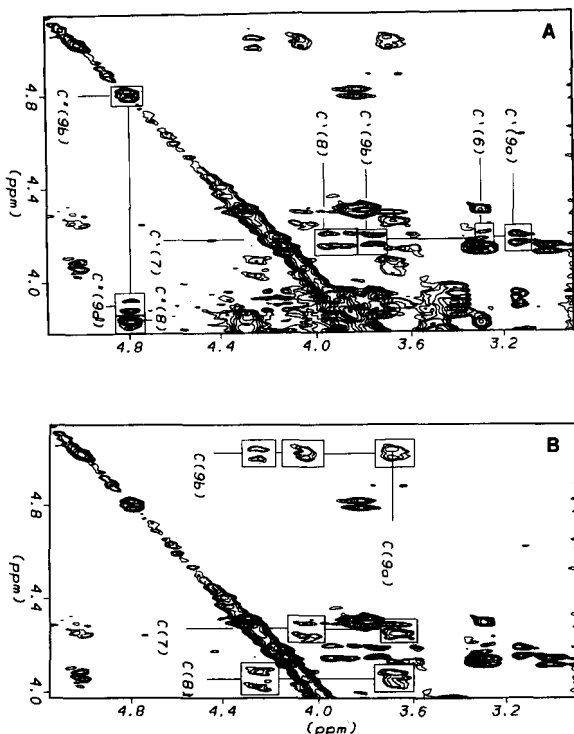


FIG. 9. A, plot of the region from the two-dimensional HOHAHA data set containing downfield shifted resonances in monoacetylated G_{D3} species. Resonances corresponding to 7-*O*-Ac G_{D3} are labeled C' while resonances corresponding to 9-*O*-Ac G_{D3} are labeled C'. B, plot of the region from the two-dimensional HOHAHA data set containing downfield shifted resonances in the diacetylated G_{D3} species. Resonances corresponding to downfield shifted protons are labeled C.

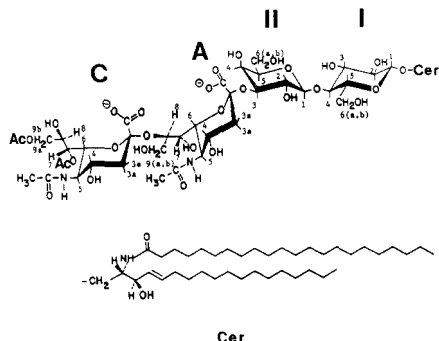


FIG. 10. The structure of di-*O*-acetylated G_{D3} purified from bovine buttermilk.

1'-Cer, 7,9-di-*O*-Ac G_{D3}). The proposed molecular structure for the di-*O*-acetyl G_{D3} is presented in Fig. 10.

DISCUSSION

Gangliosides in bovine buttermilk (Table III) are mainly present in the milk fat globule membrane which derives from the apical plasma membrane of the secretory cells in the lactating bovine mammary gland (35, 36). The ganglioside content and composition of the buttermilk have been studied by several groups (21, 33, 37, 38). In the present study, we dialyzed the buttermilk against water. This procedure not only saves organic solvents by removing effectively all small dialyzable substances, which consist of 61% by weight of the buttermilk powder, but also facilitates the recovery and purification of the gangliosides. Our data for ganglioside content and composition are different from that reported by Takamizawa *et al.* (34) who failed to detect any *O*-acetylated ganglio-

side species. The discrepancy could be due to the relative instability of the *O*-acetylated species which would have been destroyed during the base treatment step used in their ganglioside isolation procedure. Takamizawa *et al.* (34) also reported that about 90% of the gangliosides in bovine buttermilk consisted of hemato-series gangliosides, such as G_{M3} , G_{D3} , and G_{T3} . We found that about 10% of these gangliosides were acetylated on the terminal sialic acid residue. More recently, we reported the presence of *O*-acetyl G_{D3} in bovine buttermilk (21) and suggested that this is a convenient and easily available source for this ganglioside. In the present study, we have extended the previous study and found at least three *O*-acetylated gangliosides in bovine buttermilk.

Since Cheresch *et al.* (14) reported that the monoclonal antibody D1.1 recognized 9-*O*-acetyl G_{D3} on human melanoma cells, which was characterized by alkaline treatment, immunostaining, and periodate oxidation, several groups reported that the alkali-labile ganglioside migrating between G_{M1} and G_{M2} and reacting with mAb D1.1 is 9-*O*-acetyl G_{D3} (15, 21). Constantine-Paton *et al.* (6) found that the antigen recognized by JONES antibody is 9-*O*-acetylated ganglioside G_{D3} . In addition to the mAbs D1.1 and JONES, the receptor-destroying enzyme of influenza C virus, sialate *O*-acetyl esterase (39), and cancer antennarius lectin (23) can also confirm the presence of 9-*O*-acetylation on the sialic acid residues. More recently, Drazba *et al.* (40) reported that an antigen of the developing chick retina recognized by the monoclonal antibody A2B5 was a 9-*O*-acetylated ganglioside. However, none of them excluded the possibility of two acetyl groups (7 and 9) co-existing in the terminal sialic acid residue of this molecule, nor did they rule out the possibility for the presence of 7-*O*-acetyl G_{D3} which might react with these monoclonal antibodies. In the present study, the purified 7,9-*O*-diacetyl G_{D3} (G_1) and a mixture of 7-*O*-acetyl and 9-*O*-acetyl G_{D3} (G_2) from bovine buttermilk powder having a similar mobility on the HPTLC, reacted with mAbs D1.1 and JONES. All these species were converted to G_{D3} after mild alkali treatment. However, FAB-mass and NMR spectra suggested that G_1 was 7,9-*O*-diacetyl G_{D3} and G_2 a mixture of 7-*O*-acetyl and 9-*O*-acetyl G_{D3} . It should be pointed out that our resonance assignments are somewhat different from those reported by other workers (16, 22). Many of these previous assignments have relied extensively on well resolved resonances in 1H NMR spectra. On the other hand, we have relied extensively on through-bond correlated experiments for our assignment data. Thus, we are not limited to relying solely on the relatively few well resolved resonances in the 1H NMR spectra of these *O*-acetylated G_{D3} species. Given the extensive resonance overlap which characterizes the 1H NMR spectra of carbohydrates and the additional complication that the 1H NMR spectra of *O*-acetylated G_{D3} actually represents a superposition of the 1H NMR spectra of the two mono-*O*-acetylated species and the di-*O*-acetylated species, these two-dimensional experiments offer significant advantages in obtaining unambiguous resonance assignments for these compounds.

Although the difference of functional significance between 7-*O*-acetyl G_{D3} in buttermilk and 9-*O*-acetyl G_{D3} in melanoma is not yet understood, it is possible that different positions of *O*-acetylation in ganglioside might play a significant role in cell differentiation and cell growth. Dubois *et al.* (29) reported the presence of alkali-labile ganglioside G_{T3} in 10-day-old chicken embryonic retina and recently confirmed that the ganglioside is 9-*O*-acetylated G_{T3} by using immunostaining with A2B5 and 18B8 monoclonal antibodies. Hirabayashi *et al.* (41) found 9-*O*-acetyl G_{T3} in fetal rat cerebral cortex by using the receptor-destroying enzyme of influenza C virus and

TABLE III
 Gangliosides of bovine buttermilk

Ganglioside	Structure	Concentration nmol/g dry wt
G _{M3}	NeuAcα2→3Galβ1→4G1cβ1→Cer Galβ1→4G1cNacβ1	19.98
BG ^a	6(3)Galβ1→4G1cβ1→1Cer NeuAcα2→6Galβ1→4G1cNacβ1	41.40
G ₁	Ac ₂ -O-7,9NeuAcα2→8NeuAcα2→3Galβ1→4G1cβ1→1Cer	0.72
G ₂	Ac-O-7/9NeuAcα2→8NeuAcα2→3Galβ1→4G1cβ1→1Cer	13.88
G _{D3}	NeuAcα2→8NeuAcα2→3Galβ1→4G1cβ1→1Cer	204.93
G ₃	Ac-O NeuAcα2→8NeuAcα2→8NeuAcα2→3Galβ1→4G1cβ1→1Cer	11.87
G _{T3}	NeuAcα2→8NeuAcα2→8NeuAcα2→3Galβ1→4G1cβ1→1Cer	12.73

^a Cited from Ref. 34.

base treatment. The precise chemical structures of these gangliosides, however, have not been carefully examined. In this investigation, we found and characterized the O-acetyl G_{T3} in bovine buttermilk by using chemical and immunological methods and provided conclusive evidence that the O-acetyl group is present at the terminal sialic acid residue. Because of its reactivity with mAb A2B5, but not with mAb 18B8, it suggests that the position of the acetyl group is most likely to be at the 9- and/or 7-O-position on the terminal sialic acid residue. The data also suggest that the free terminal sialic acid residue is important for the interaction of G_{T3} with mAb 18B8. These results are consistent with those reported from chicken embryonic retina (29). Further studies are needed to clarify the position of the O-acetyl group in O-acetylated G_{T3}. Nonetheless, this is also the first report for the presence of O-acetyl G_{T3} in bovine buttermilk. Since buttermilk is commercially available, it represents a convenient source for the isolation of this ganglioside.

O-Acetylated gangliosides, including 7-O-acetyl G_{D3}, 9-O-acetyl G_{D3}, 7,9-di-O-acetyl G_{D3}, and O-acetylated G_{T3} increase the possible number of these molecular species leading to a larger diversity in the pattern of cell surface gangliosides. Although these species have been described originally in developing rat and chicken nervous systems, and human melanomas several years ago, functional studies have been scanty so far. The availability of large quantities of O-acetylated gangliosides from bovine buttermilk would facilitate greatly the study of the function of O-acetylated gangliosides in cellular differentiation and development.

REFERENCES

- Svennerholm, L. (1964) *J. Lipid Res.* **5**, 145-162
- IUPAC-IUB Commission of Biochemical Nomenclature (1978) *Biochem. J.* **171**, 21-35
- Rosenberg, A., and Schengrund, C. (1976) *Biological Roles of Sialic Acid*, Plenum Publishing Corp., New York
- Schauer, R. (1982) *Cell Biol. Monogr.* **10**, 32-39
- Levine, J. M., Beasley, L., and Stallcup, W. B. (1986) *Dev. Brain Res.* **27**, 211-222
- Constantine-Paton, M., Blum, A. S., Mendez-Otero, R., and Barnstable, C. J. (1986) *Nature* **324**, 459-462
- Muchmore, E., and Varki, A. (1987) *Science* **236**, 1293-1295
- Sparrow, J. R., and Barnstable, C. J. (1988) *J. Neurosci.* **8**, 580-592
- Schlosshauer, B., Blum, A. S., Mendez-Otero, R., Barnstable, C. J., and Constantine-Paton, M. (1988) *J. Neurosci.* **8**, 580-592
- Mendez-Otero, R., Schlosshauer, B., Barnstable, C. J., and Constantine-Paton, M. (1988) *J. Neurosci.* **8**, 564-579
- Chou, D. K. H., Flores, S., and Jungalwala, F. B. (1990) *J. Neurochem.* **54**, 1598-1607
- Reid, P. E., Culling, C. F., Dunn, W. L., Ramey, C. W., and Clay, M. G. (1984) *Histochem. J.* **16**, 235-251
- Cheresh, D. A., Reisfeld, R. A., and Varki, A. (1984) *Science* **225**, 844-846
- Cheresh, D. A., Varki, A., Varki, N. M., Stallcup, W. B., Levine, J., and Reisfeld, R. A. (1984) *J. Biol. Chem.* **259**, 7453-7459
- Levine, J., Beasley, L., and Stallcup, W. (1984) *J. Neurosci.* **4**, 820-831
- Thurin, J., Herlyn, M., Hindsgaul, O., Stromberg, N., Karlsson, K. A., Elder, D., Stepkowski, Z., and Koprowski, H., (1985) *J. Biol. Chem.* **260**, 14556-14563
- Blum, A. S., and Barnstable, C. J. (1987) *Proc. Natl. Acad. Sci. U. S. A.* **84**, 8716-8720
- Stallcup, W. B., Pytela, R., and Ruoslahti, E. (1989) *Dev. Biol.* **132**, 212-229
- Varki, A., Hooshmand, F., Diaz, S., Varki, N. M., and Hedrick, S. M. (1991) *Cell* **65**, 65-74
- Ren, S. L., Slominski, A., and Yu, R. K. (1989) *Cancer Res.* **49**, 7051-7056
- Bonafede, D., Macala, L. J., Constantine-Paton, M., and Yu, R. K. (1989) *Lipids* **24**, 680-684
- Ostrander, G. K., Bozlee, M., Fukuda, M., Dell, A., Thomas-Oates, J. E., Levery, S. B., Eaton, H. L., Hakomori, S. I., and Holmes, E. H. (1991) *Arch. Biochem. Biophys.* **284**, 413-421
- Ravindranath, M. H., Paulson, J. C., and Irie, R. F. (1984) *J. Biol. Chem.* **259**, 2079-2086
- Ritter, G., Boosefeld, E., Markstein, E., Yu, R. K., Ren, S. L., Stallcup, W. B., Oettgen, H. F., Old, L. J., and Livingston, P. O. (1990) *Cancer Res.* **50**, 1403-1410
- Ledeer, R., and Yu, R. K. (1982) *Methods Enzymol.* **83**, 139-191
- Folch, J., Lees, M., and Sloane-Stanley, G. H. (1957) *J. Biol. Chem.* **226**, 139-191
- Svennerholm, L. (1957) *Biochim. Biophys. Acta* **24**, 604-611
- Kasai, N., Naiki, M., and Yu, R. K. (1984) *J. Biochem. (Tokyo)* **96**, 261-264
- Dubois, C., Manuguerra, J. C., Hauttecoeur, B., and Maze, J. (1990) *J. Biol. Chem.* **265**, 2797-2803
- Kasai, N., and Yu, R. K. (1983) *Brain Res.* **277**, 155-158
- Ariga, T., Macala, L. J., Saito, M., Margolis, R. K., Greene, L. A., Margolis, R. U., and Yu, R. K. (1988) *Biochemistry* **27**, 52-58
- Yu, R. K., Koerner, T. A. W., Scarsdale, J. N., and Prestegard, J. H. (1986) *Chem. Phys. Lipids* **42**, 27-48
- Ando, S., Yu, R. K., Scarsdale, J. N., Kusunoki, S., and Prestegard, J. H. (1989) *J. Biol. Chem.* **264**, 3478-3483
- Takamizawa, K., Iwamori, M., Mutai, M., and Nagai, Y. (1986) *J. Biol. Chem.* **261**, 5625-5630
- Patton, S., and Keenan, T. W. (1975) *Biochim. Biophys. Acta* **415**, 273-309
- McPherson, A. V., and Kitchen, B. J. (1983) *J. Dairy Res.* **50**, 107-133
- Keenan, T. W. (1974) *Biochim. Biophys. Acta* **337**, 255-270
- Huang, R. T. C. (1973) *Biochim. Biophys. Acta* **306**, 82-84
- Rogers, G. N., Herrler, G., Paulson, J. C., and Klenk, H. D. (1986) *J. Biol. Chem.* **261**, 5947-5951
- Drazba, J., Pierce, M., and Lemmon, V. (1991) *Dev. Biol.* **145**, 154-163
- Hirabayashi, Y., Hirota, M., Suzuki, Y., Matsumoto, M., Obata, K., and Ando, S. (1989) *Neurosci. Lett.* **106**, 193-198